Multiphysics Degradation Modeling of Energy Storage Materials via RKPM with a Neural Network-Enhancement

Kristen Susuki[1]

Advisor: J.S. Chen[1]

Collaborators: Jeff Allen[2]

[1] University of California San Diego, Department of Structural Engineering
[2] National Renewable Energy Laboratory, Computational Science Center

UC San Diego NREL Transforming ENERGY

EMI Conference – Chicago, IL – May 30, 2024
NREL/PR-2C00-89940

Li-ion Battery Electrode Microstructures and Electro-Chemo-Mechanical Cracking

Electrode Microstructure and Electro-Chemo-Mechanical Cracking

Cathode Composition:
- Randomly-oriented grains
- Anisotropic grain material properties

Charge Cycling:
- Lithium movement between electrodes causes nonuniform grain expansion and contraction

Electro-chemo-mechanical cracking:
- Inhibited lithium flow via tortuous diffusion path
- Reduced battery life

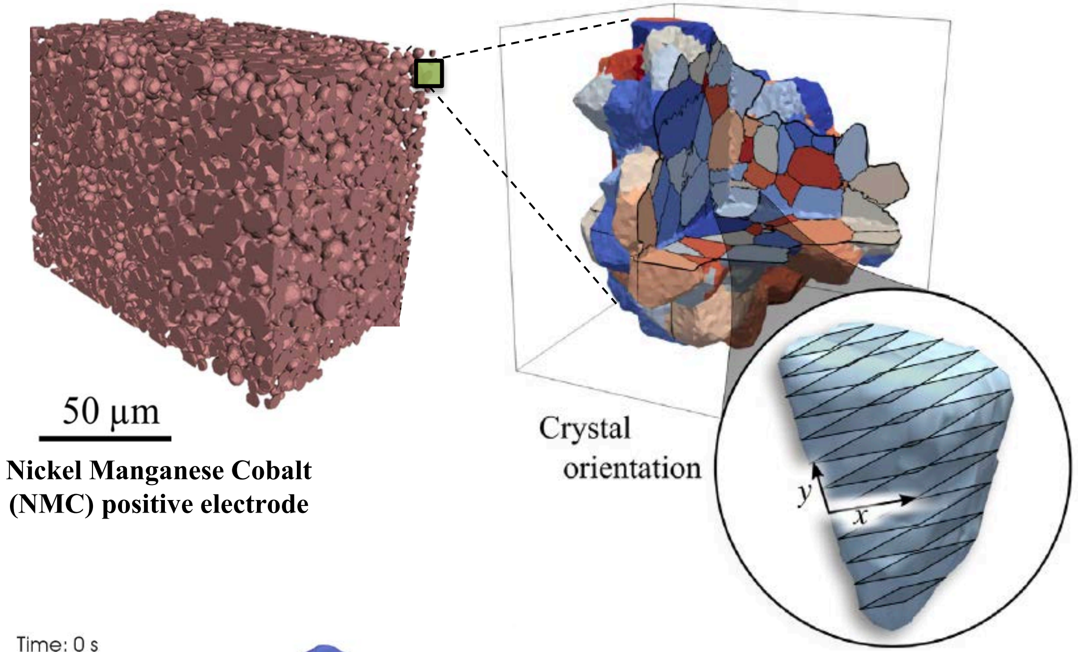

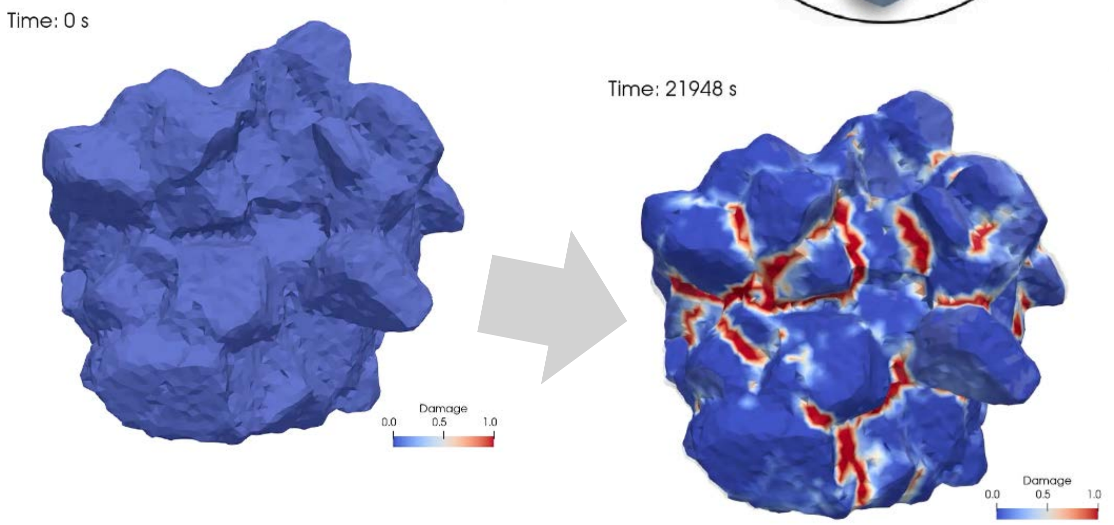

1. NREL. "Battery Microstructures Library." https://www.nrel.gov/transportation/microstructure.html.
2. Allen, J., P. Weddle, A. Verma, et al. 2021. "Quantifying the influence of charge rate and cathode-particle architectures on degradation of Li-ion cells through 3D continuum-level damage models." *J. Power Sources*.
3. Quinn, A., H. Moutinho, F. Usseglio-Viretta, et al. 2020. "Electron Backscatter Diffraction for Investigating Lithium-Ion Electrode Particle Architectures." *Cell Rep Phys Sci* 1, 100137.

Governing Equations

Electrochemical Model

c

Lithium transport balance → lithium concentration c

$$\dot{c} + \nabla \cdot \boldsymbol{J} = 0 \quad in\ \Omega$$
$$\boldsymbol{J} = -\boldsymbol{D} \cdot \nabla c$$
$$\boldsymbol{D} \cdot \nabla c \cdot \boldsymbol{n} = -\frac{\bar{J}(c, \Phi)}{F} \quad on\ \Gamma_{h_c}$$

Φ

Solid-phase electrostatic potential balance → potential Φ

$$\nabla \cdot (\kappa \nabla \Phi) = 0 \quad in\ \Omega$$
$$\kappa \nabla \Phi \cdot \boldsymbol{n} = -\left(\bar{J}(c, \Phi) + \bar{J}_{applied}\right) \quad on\ \Gamma_{h_\Phi}$$

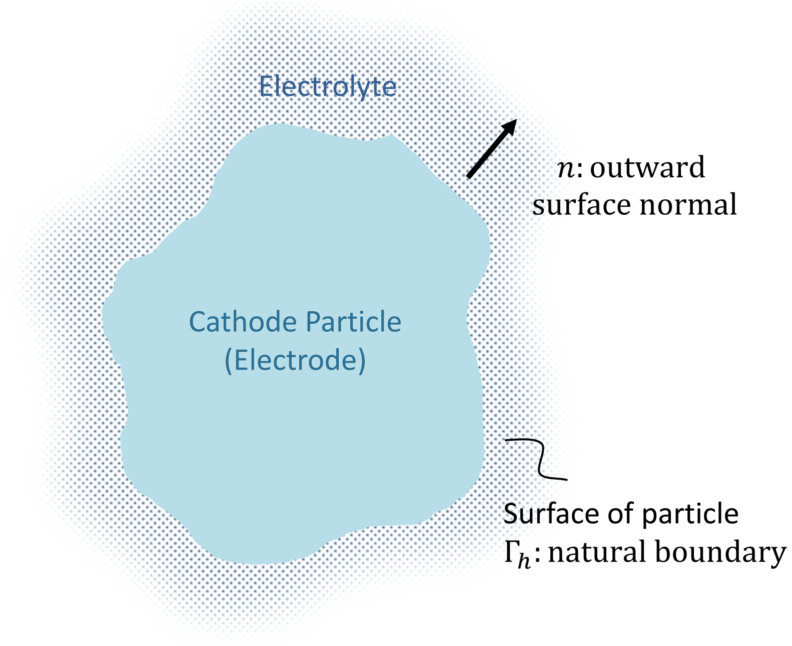

Mechanical Model

$\boldsymbol{u}$

Diffusion-induced mechanical deformation → displacement $\boldsymbol{u}$

$$\nabla \cdot \boldsymbol{\sigma} = \boldsymbol{0} \quad in\ \Omega$$
$$\boldsymbol{\sigma} = \mathbb{C}\boldsymbol{\epsilon}^e$$
$$\boldsymbol{\sigma} \cdot \boldsymbol{n} = 0 \quad on\ \Gamma_{h_u}$$
$$\boldsymbol{\epsilon}^e = \boldsymbol{\epsilon} - \boldsymbol{\epsilon}^D$$
$$\boldsymbol{\epsilon}^D = \boldsymbol{\beta}\Delta C$$

Butler-Volmer interface condition

$$\bar{J}(c, \Phi) = \bar{J}_0 \left[\exp\left(\frac{\alpha_a \eta F}{RT}\right) - \exp\left(-\frac{\alpha_c \eta F}{RT}\right)\right]$$
$$\eta(c, \Phi) = \Phi - \Phi_{el} - E^{eq}\left(\frac{c}{c_{max}}\right)$$

4. G.L. Plett, Battery Management Systems, Volume I: Battery Modeling, Artech House, 2015.
5. Doyle, M., T. Fuller, J. Newman, "Modeling of Galvanistic Charge and Discharge of the Lithium/Polymer/Insertion Cell", *Journal of the Electrochemical Society*. 140 (1993).
6. Richardson, G.W. , J.M. Foster, R. Ranom, C.P. Please, A.M. Ramos, "Charge transport modelling of Lithium-ion batteries", *Eur. J. Appl. Math*. 33 (2022).

Reproducing Kernel Particle Method (RKPM)

Reproducing Kernel (RK) Approximation

RK Approximation:

$$u(\boldsymbol{x}) \approx u^h(\boldsymbol{x}) = \sum_{I=1}^{NP} \Psi_I(\boldsymbol{x}) d_I$$

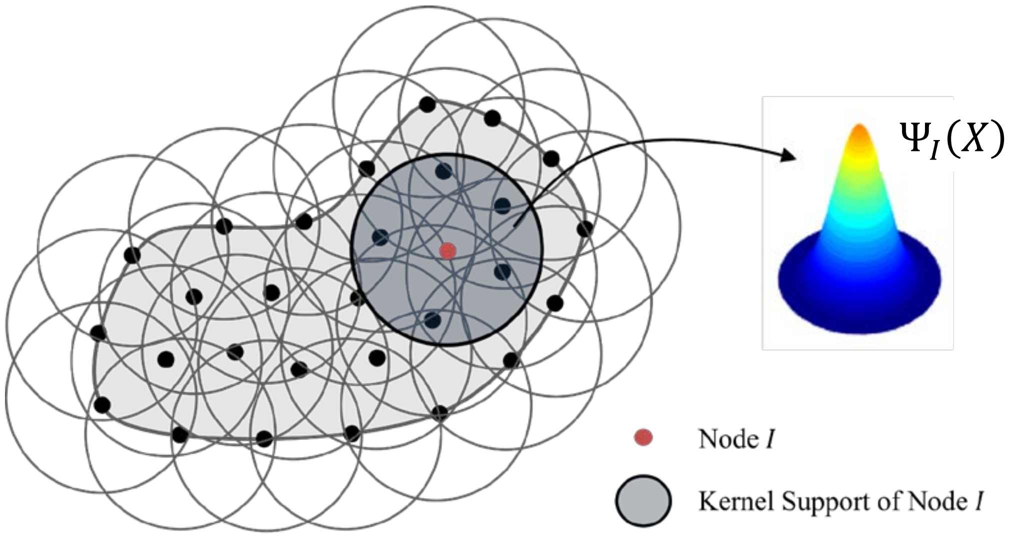

Shape Function Construction: $\Psi_I(\boldsymbol{x})$

Strategic Correction of Kernel Functions, ϕ_a :

$$\Psi_I(\boldsymbol{x}) = C(\boldsymbol{x}; \boldsymbol{x} - \boldsymbol{x}_I)\phi_a(\boldsymbol{x} - \boldsymbol{x}_I) = \left(\sum_{|\boldsymbol{\alpha}|\le n} (\boldsymbol{x} - \boldsymbol{x}_I)^{\boldsymbol{\alpha}} b_{\boldsymbol{\alpha}}(\boldsymbol{x})\right) \phi_a(\boldsymbol{x} - \boldsymbol{x}_I)$$

$$\Psi_I(\boldsymbol{x}) \equiv \boldsymbol{H}^T(\boldsymbol{x} - \boldsymbol{x}_I)\ \boldsymbol{b}(\boldsymbol{x})\ \phi_a(\boldsymbol{x} - \boldsymbol{x}_I)$$

controls order of **completeness**

ensures satisfaction of **reproducing conditions**

controls order of **continuity**

$$\boldsymbol{H}^T(\boldsymbol{x} - \boldsymbol{x}_I) = [1, (x_1 - x_{1I}), (x_2 - x_{2I}), (x_3 - x_{3I}), \ldots, (x_3 - x_{3I})^n]$$

$$\boldsymbol{b}(\boldsymbol{x}) = \boldsymbol{M}^{-1}(\boldsymbol{x})\boldsymbol{H}(\boldsymbol{0}),\quad where\ \mathbf{M}(\boldsymbol{x}) = \sum_{I=1}^{NP} \mathbf{H}(\boldsymbol{x} - \boldsymbol{x}_I)\mathbf{H}^{\mathrm{T}}(\boldsymbol{x} - \boldsymbol{x}_I)\phi_a(\boldsymbol{x} - \boldsymbol{x}_I)$$

7. Liu, W.K., S. Jun, S. Li, J. Adee, T. Belytschko. 1995. “Reproducing kernel particle methods for structural dynamics.” *Int J Numer Methods Eng* 38(10): 1655-1679.
8. Chen, J.S., C. Pan, C-T Wu, W.K. Liu. 1996. “Reproducing kernel particle methods for large deformation analysis of non-linear structures.” *Comput Methods Appl Mech Eng* 139(96): 195-227.

Patch Test for Coupled Electro-Chemo-Mechanical Problem

Coupled Linear Patch Test Construction

Let’s define a coupled BVP where the source term and BCs are associated with predefined fields.

⬇

The solution fields in the domain interior are expected to reproduce the predefined fields.

Predefined Fields:

$c^p = 34720 + 2480x_1 + 7440x_2$

$\Phi^p = 3.8285 - 0.05x_1 - 0.1x_2$

$u_1^p = 10^{-1}\, x_1$

$u_2^p = 2\text{x}10^{-1}\, x_2$

Butler-Volmer interface condition

$$\bar{J}(c,\Phi) = \bar{J}_0\left[\exp\left(\frac{\alpha_a \eta F}{RT}\right) - \exp\left(-\frac{\alpha_c \eta F}{RT}\right)\right] \quad on\ \Gamma_h$$

$$\eta(c,\Phi) = \Phi - \Phi_{el} - E^{eq}\left(\frac{c}{c_{max}}\right)$$

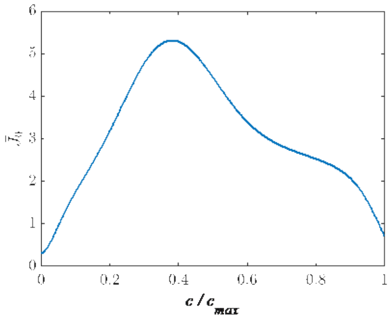

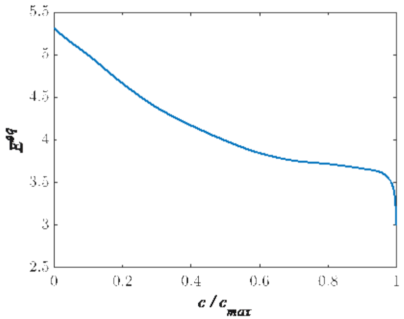

Governing equations:

$$\nabla\cdot(-\boldsymbol{D}\cdot\nabla c) = s^c \qquad in\ \Omega$$
$$\nabla\cdot(\kappa\nabla\Phi) = s^\Phi \qquad in\ \Omega$$
$$\nabla\cdot\boldsymbol{\sigma} = \boldsymbol{s}^u \qquad in\ \Omega$$

Boundary conditions:

$$D\,\nabla c\cdot\boldsymbol{n} = D\,\nabla c^p\cdot\boldsymbol{n} + \frac{\bar{J}^p(c^p,\Phi^p)}{F} - \frac{\bar{J}}{F} \qquad on\ \Gamma_{h_c} = \Gamma$$

$$\kappa\,\nabla\Phi\cdot\boldsymbol{n} = \kappa\nabla\Phi^p\cdot\boldsymbol{n} + \bar{J}^p(c^p,\Phi^p) - \bar{J} \qquad on\ \Gamma_{h_\Phi} = \Gamma$$

$$\boldsymbol{\sigma}\cdot\boldsymbol{n} = 0 \qquad on\ \Gamma_{h_u} = \Gamma$$

Source terms: $s^c = 0;\quad s^\Phi = 0;\quad \boldsymbol{s}^u = \boldsymbol{0}$

9. **Susuki, K.**, J. Allen, J.S. Chen. 2024. “Image-based Modeling of Coupled Electro-Chemo-Mechanical Behavior of Li-ion Battery Cathode Using an Interface-Modified Reproducing Kernel Particle Method.” *Eng Comput* (Submitted)

Linear Patch Test Results for Coupled Electro-Chemo-Mechanical Problem

Relative Error Norm Equations

$\boldsymbol{L_2}$ **Norm:**

$$\| f - f^h \|_0 = \frac{\left(\int_\Omega \left(f - f^h\right)^2 d\Omega\right)^{\frac{1}{2}}}{\left(\int_\Omega f^2 d\Omega\right)^{\frac{1}{2}}}$$

$$\| \boldsymbol{f} - \boldsymbol{f}^h \|_0 = \frac{\left(\int_\Omega \left(f_i - f_i^h\right)^2 d\Omega\right)^{\frac{1}{2}}}{\left(\int_\Omega f_i^2 d\Omega\right)^{\frac{1}{2}}}$$

$\boldsymbol{H^1}$ **Semi-Norm:**

$$\left|f - f^h\right|_1 = \frac{\left(\int_\Omega \left(f_{,i} - f_{,i}^h\right)^2 d\Omega\right)^{\frac{1}{2}}}{\left(\int_\Omega f_{,i}^2 d\Omega\right)^{\frac{1}{2}}}$$

$$\left|\boldsymbol{f} - \boldsymbol{f}^h\right|_1 = \frac{\left(\int_\Omega \left(f_{i,j} - f_{i,j}^h\right)^2 d\Omega\right)^{\frac{1}{2}}}{\left(\int_\Omega {f_{i,j}}^2 d\Omega\right)^{\frac{1}{2}}}$$

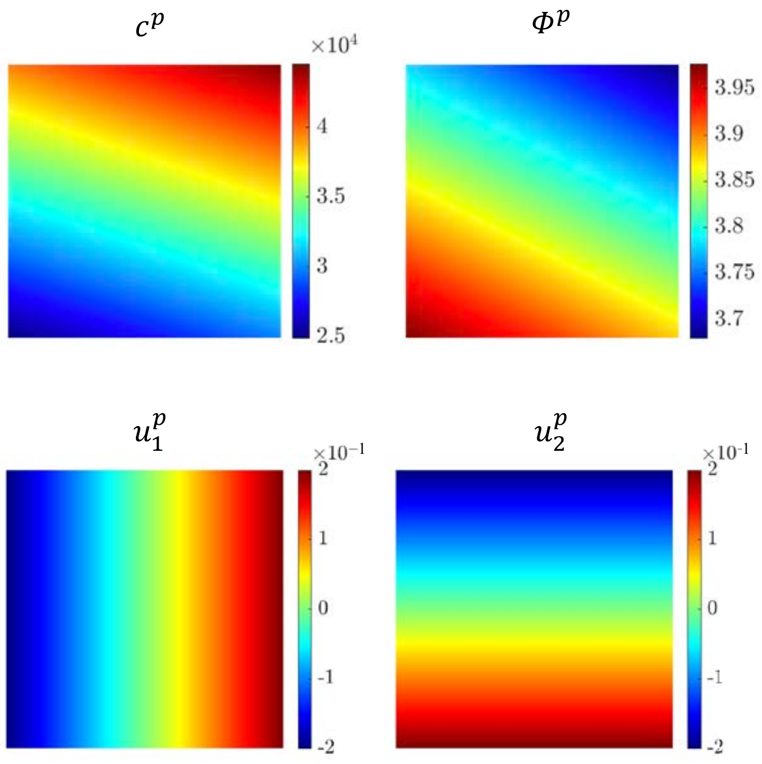

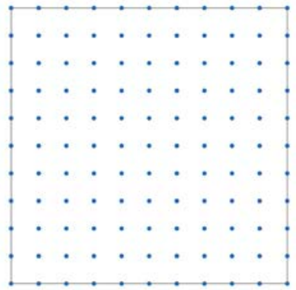

Note: Eigenvalue shifting used to suppress rigid modes

Field	Relative Error L_2 Norm	Relative Error H^1 Semi-norm
c	$1.23x10^{-14}$	$1.29x10^{-13}$
Φ	$5.96x10^{-15}$	$5.05x10^{-13}$
$\boldsymbol{u}$	$8.21x10^{-11}$	$8.02x10^{-10}$

9. **Susuki, K.**, J. Allen, J.S. Chen. 2024. "Image-based Modeling of Coupled Electro-Chemo-Mechanical Behavior of Li-ion Battery Cathode Using an Interface-Modified Reproducing Kernel Particle Method." *Eng Comput* (Submitted)

Mesh Convergence Study of High-Order Manufactured Solution

Mesh Convergence Study of High-Order Solution

Manufactured Fields:

$$c^p = a_0 + A^c cos(i\pi x_1)\cos(j\pi x_2)$$

$$\Phi^p = b_0 + A^\Phi cos(i\pi x_1)\cos(j\pi x_2)$$

$$u_1^p = \frac{\beta_1 A^c}{i\pi} sin(i\pi x_1)\cos(j\pi x_2)$$

$$u_2^p = \frac{\beta_2 A^c}{j\pi} sin(i\pi x_1)\cos(j\pi x_2)$$

Frequency: $i = j = 2$

Relative Error L_2 Norm

Theoretical L_2 Convergence Rate: 2

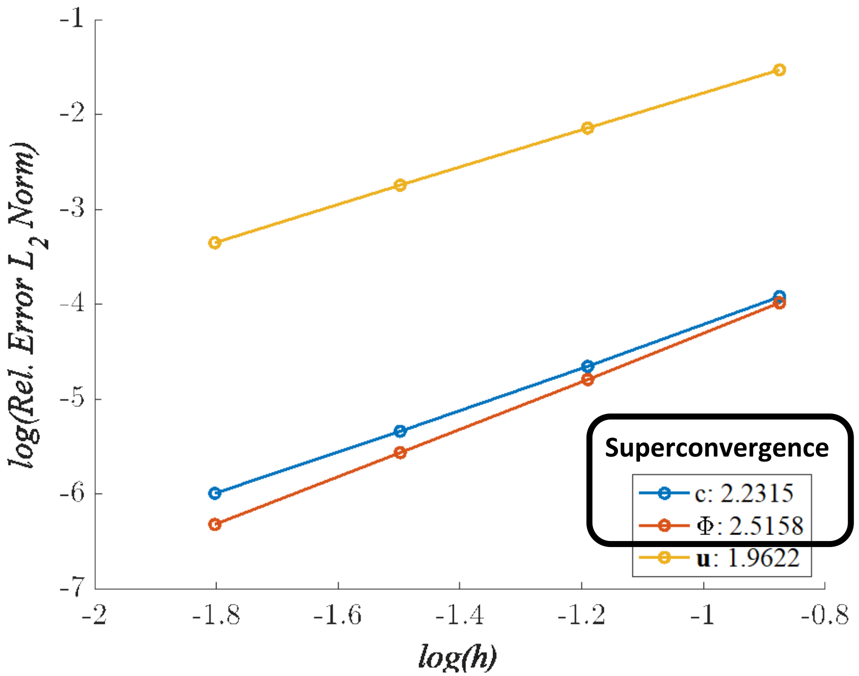

Relative Error H^1 Semi-Norm

Theoretical H^1 Convergence Rate: 1

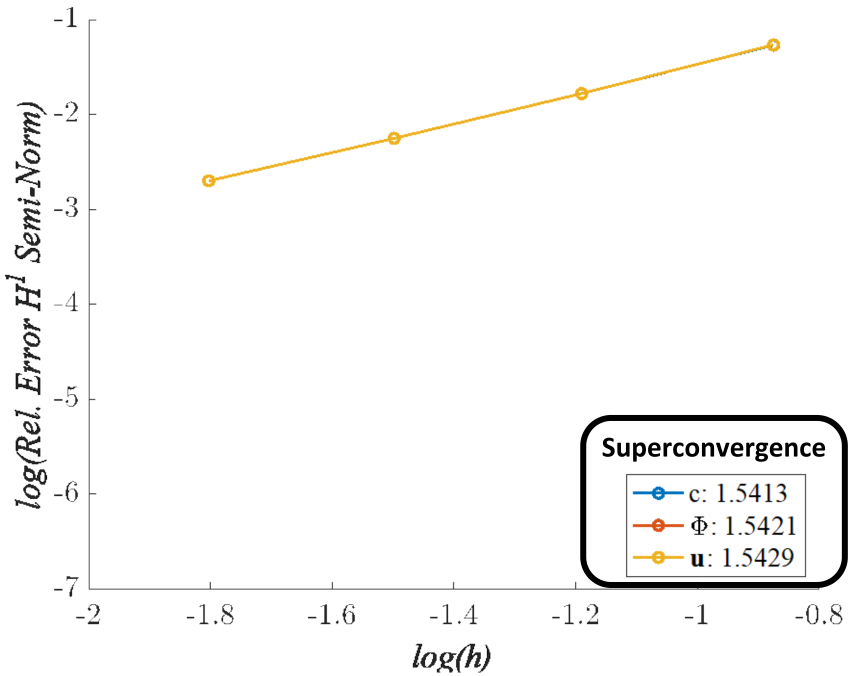

9. **Susuki, K.**, J. Allen, J.S. Chen. 2024. “Image-based Modeling of Coupled Electro-Chemo-Mechanical Behavior of Li-ion Battery Cathode Using an Interface-Modified Reproducing Kernel Particle Method.” *Eng Comput* (Submitted)

UC San Diego
Jacobs School of Engineering

Interface-Modified RK (IM-RK) Approximation for Weak and Strong Discontinuities

Interface-Modified RK (IM-RK) Approximation for Weak and Strong Discontinuities

$\bar{\Psi}_I(\boldsymbol{X})$: IM-RK Shape Functions for Neighboring Nodes

C^2 continuity, boundary conforming

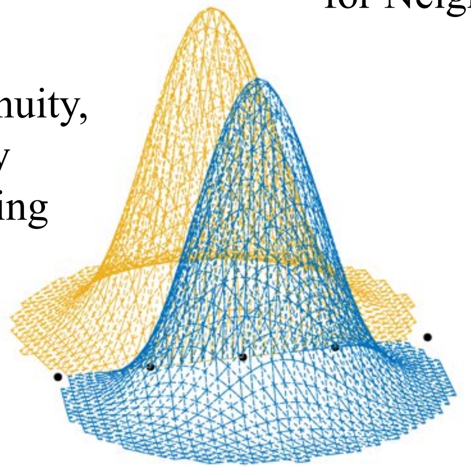

$\Psi_I(\boldsymbol{X})$: RK Shape Function for Bulk Nodes

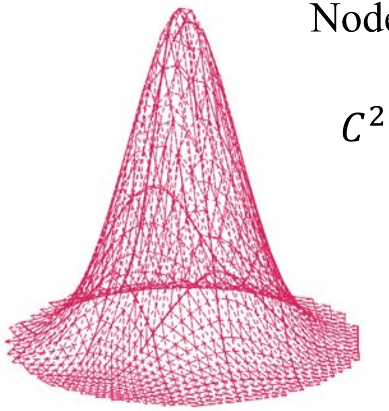

C^2 continuity

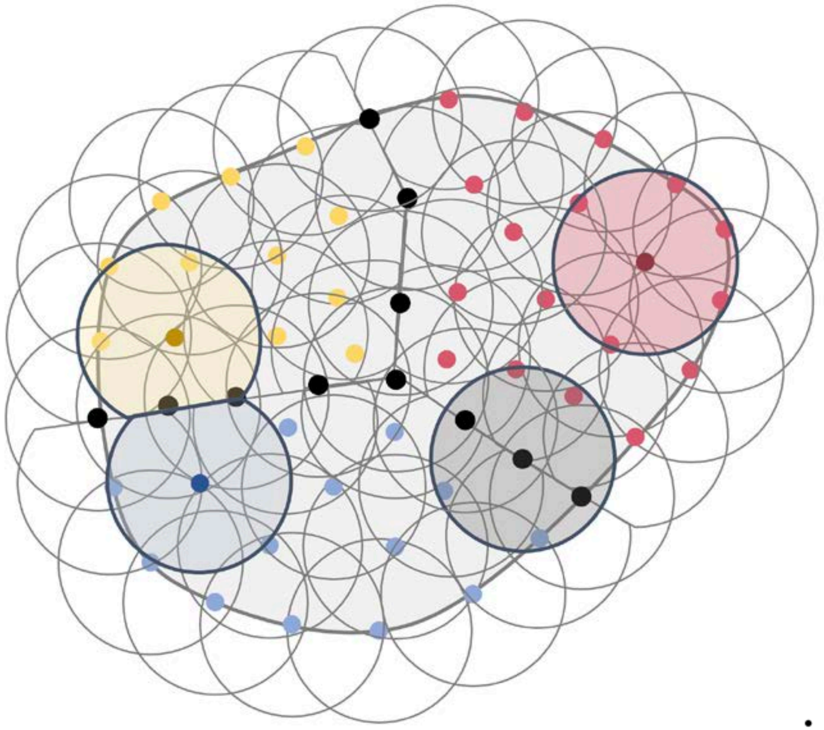

- Bulk Nodes
- Grain Boundary Nodes
- Neighboring Nodes
- Neighboring Nodes
- Kernel Support of Nodes

Note: C^{-1} continuity can also be easily achieved

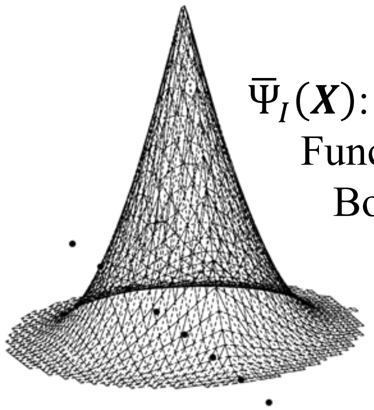

$\bar{\Psi}_I(\boldsymbol{X})$: IM-RK Shape Function for Grain Boundary Nodes

C^0 continuity

9. **Susuki, K.**, J. Allen, J.S. Chen. 2024. "Image-based Modeling of Coupled Electro-Chemo-Mechanical Behavior of Li-ion Battery Cathode Using an Interface-Modified Reproducing Kernel Particle Method." *Eng Comput* (Submitted)

10. Wang, Y., J. Baek, Y. Tang, J. Du, M. Hillman, J.S. Chen. 2023. "Support vector machine guided reproducing kernel particle method for image-based modeling of microstructures", *Computational Mechanics*.

Kernel Function Modifications for Grain Boundaries: $\max[\tanh(dist), 0]$

***IM-RK with Weak Discontinuity**: Scaling with node on interface*

Weak discontinuity introduced only for $\bar{\Psi}_{Interface}$

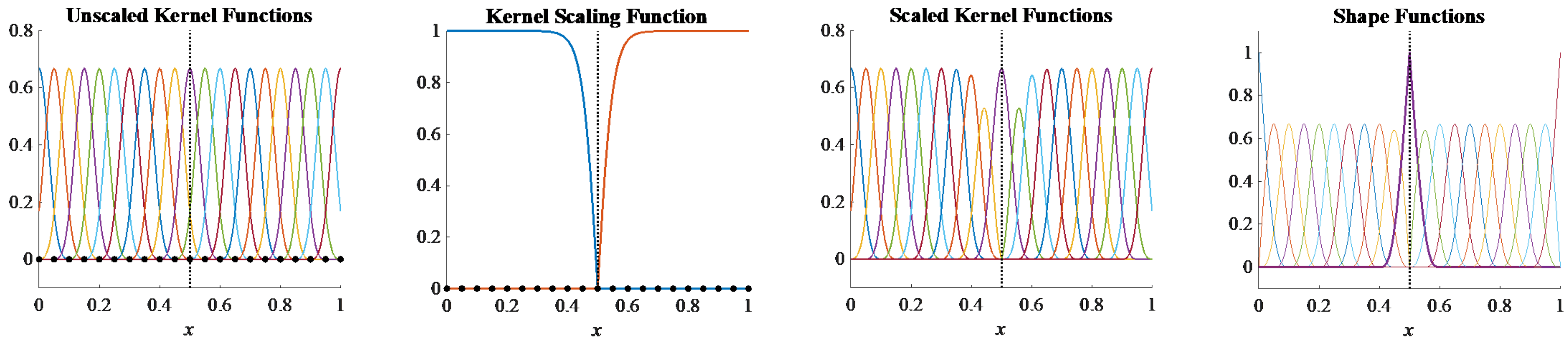

***IM-RK with Strong Discontinuity**: Scaling with no node on interface*

Strong discontinuity introduced only for $\bar{\Psi}_{Interface}$

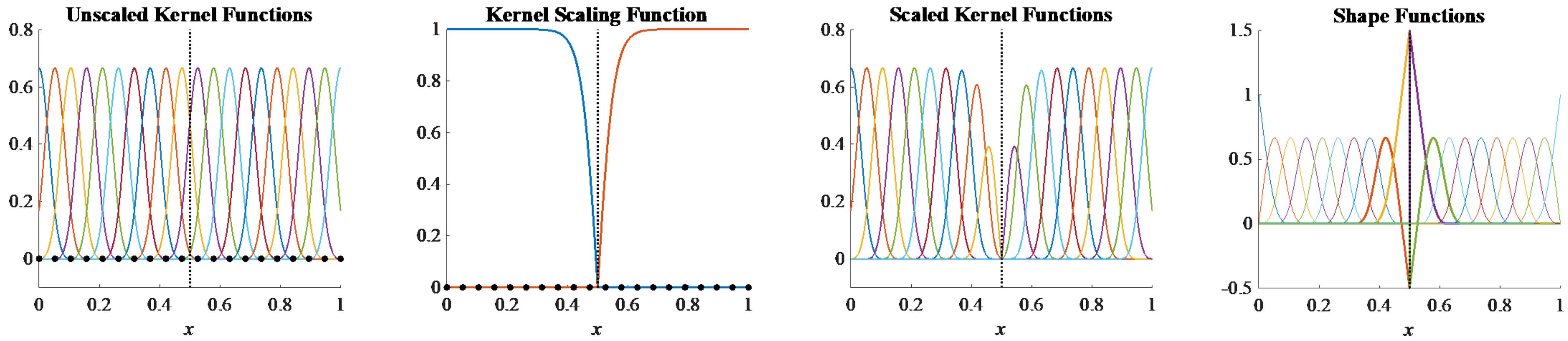

9. **Susuki, K.**, J. Allen, J.S. Chen. 2024. "Image-based Modeling of Coupled Electro-Chemo-Mechanical Behavior of Li-ion Battery Cathode Using an Interface-Modified Reproducing Kernel Particle Method." *Eng Comput* (Submitted)

10. Wang, Y., J. Baek, Y. Tang, J. Du, M. Hillman, J.S. Chen. 2023. "Support vector machine guided reproducing kernel particle method for image-based modeling of microstructures", *Computational Mechanics*.

UC San Diego
Jacobs School of Engineering

Function Approximation, u^h

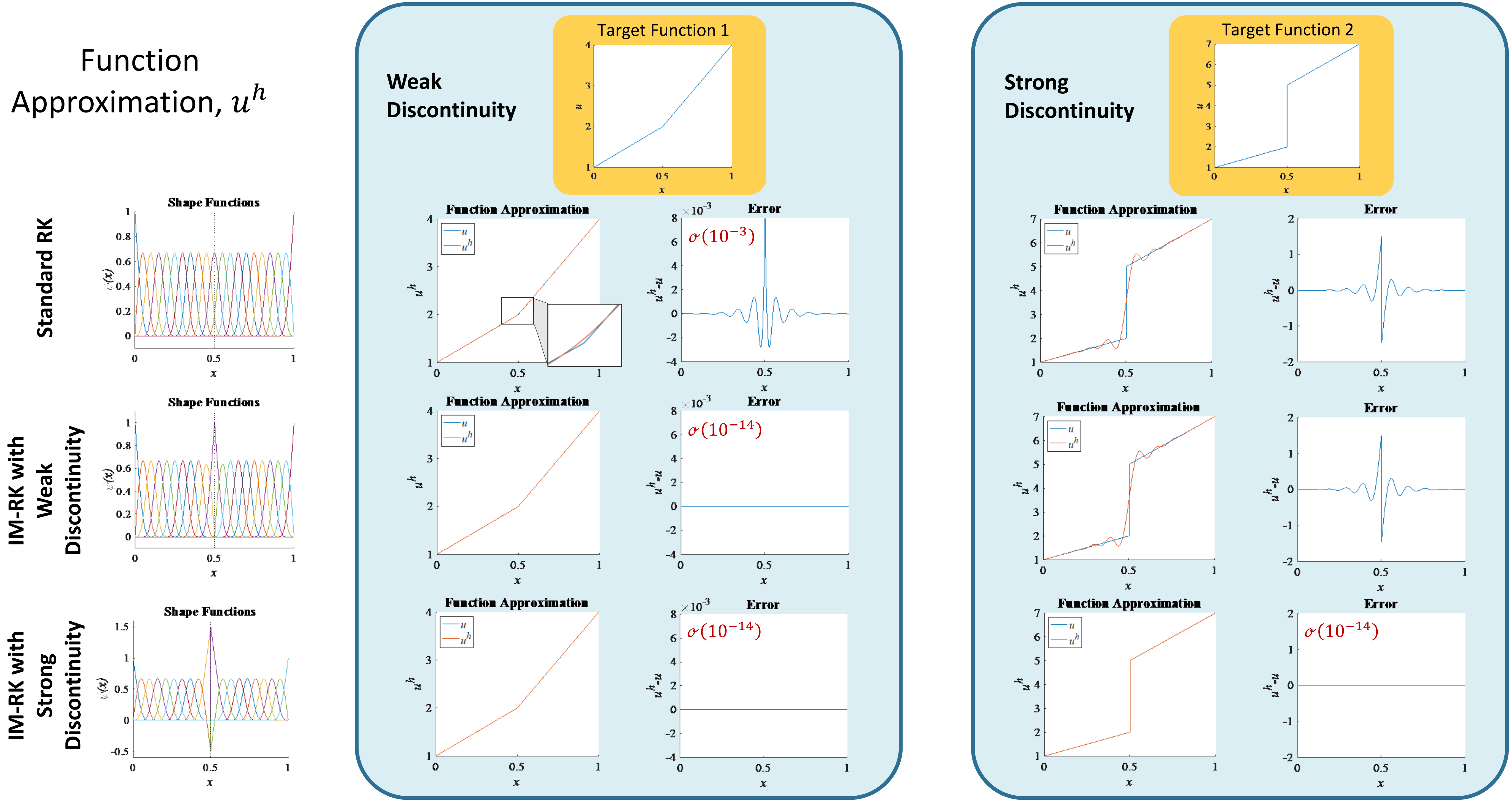

9. **Susuki, K.**, J. Allen, J.S. Chen. 2024. "Image-based Modeling of Coupled Electro-Chemo-Mechanical Behavior of Li-ion Battery Cathode Using an Interface-Modified Reproducing Kernel Particle Method." *Eng Comput* (Submitted)

Image-Based Modeling of Statistically-Driven Li-ion Battery Microstructures

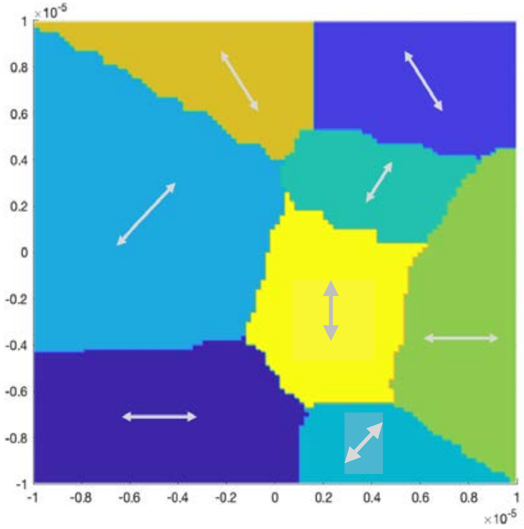

Standard RK

IM-RK

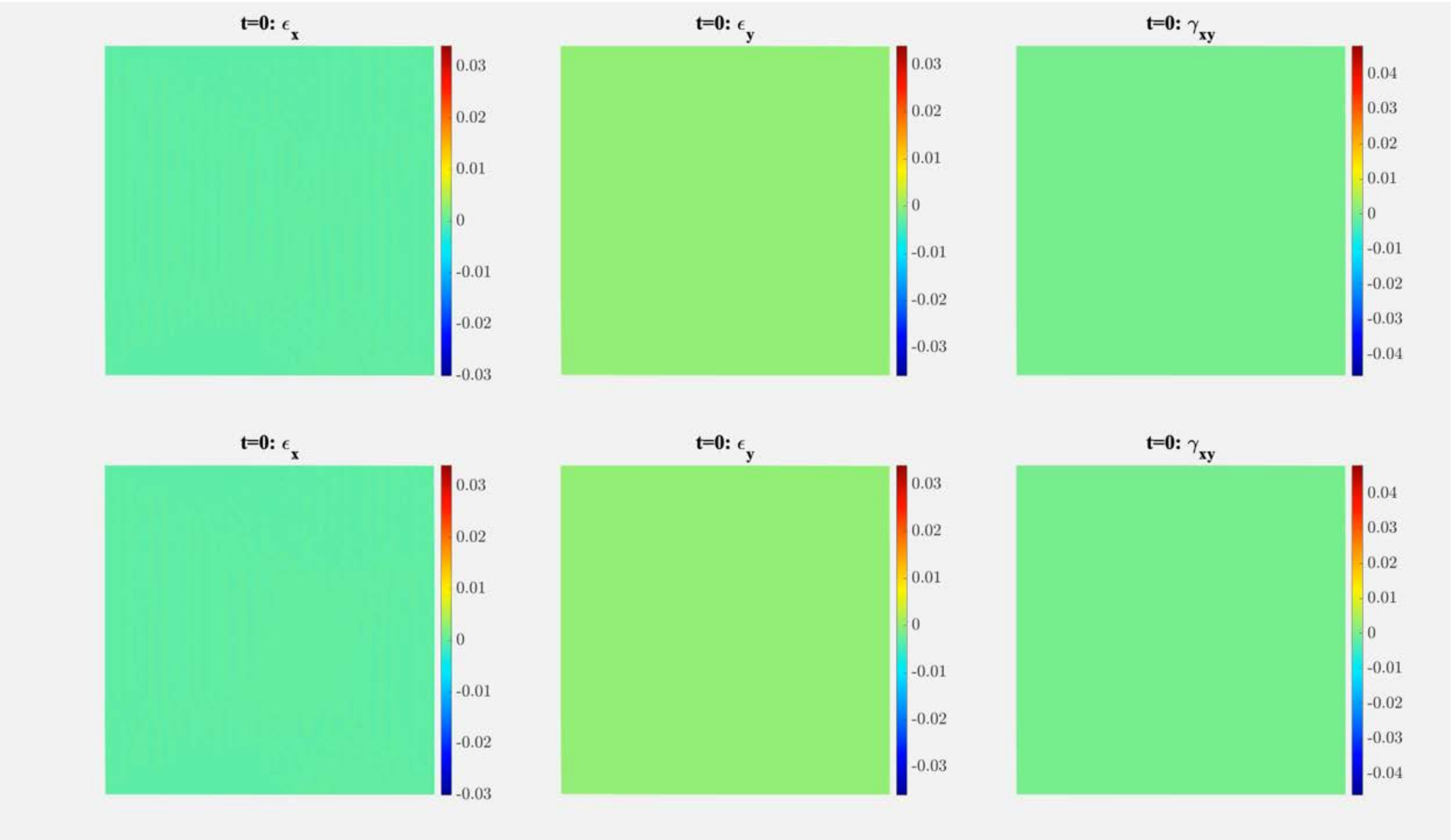

9. **Susuki, K.**, J. Allen, J.S. Chen. 2024. "Image-based Modeling of Coupled Electro-Chemo-Mechanical Behavior of Li-ion Battery Cathode Using an Interface-Modified Reproducing Kernel Particle Method." *Eng Comput* (Submitted)
11. Furat, O., L. Petrich, D. Finegan, et al. 2021. "Artificial generation of representative single Li-ion electrode particle architectures from microscopy data." *npj Computational Materials*.

UC San Diego
Jacobs School of Engineering

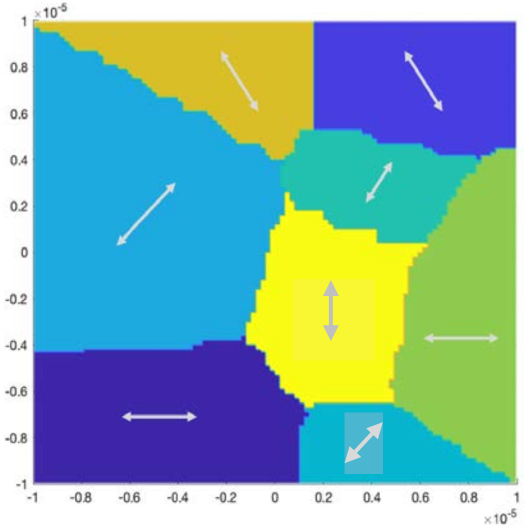

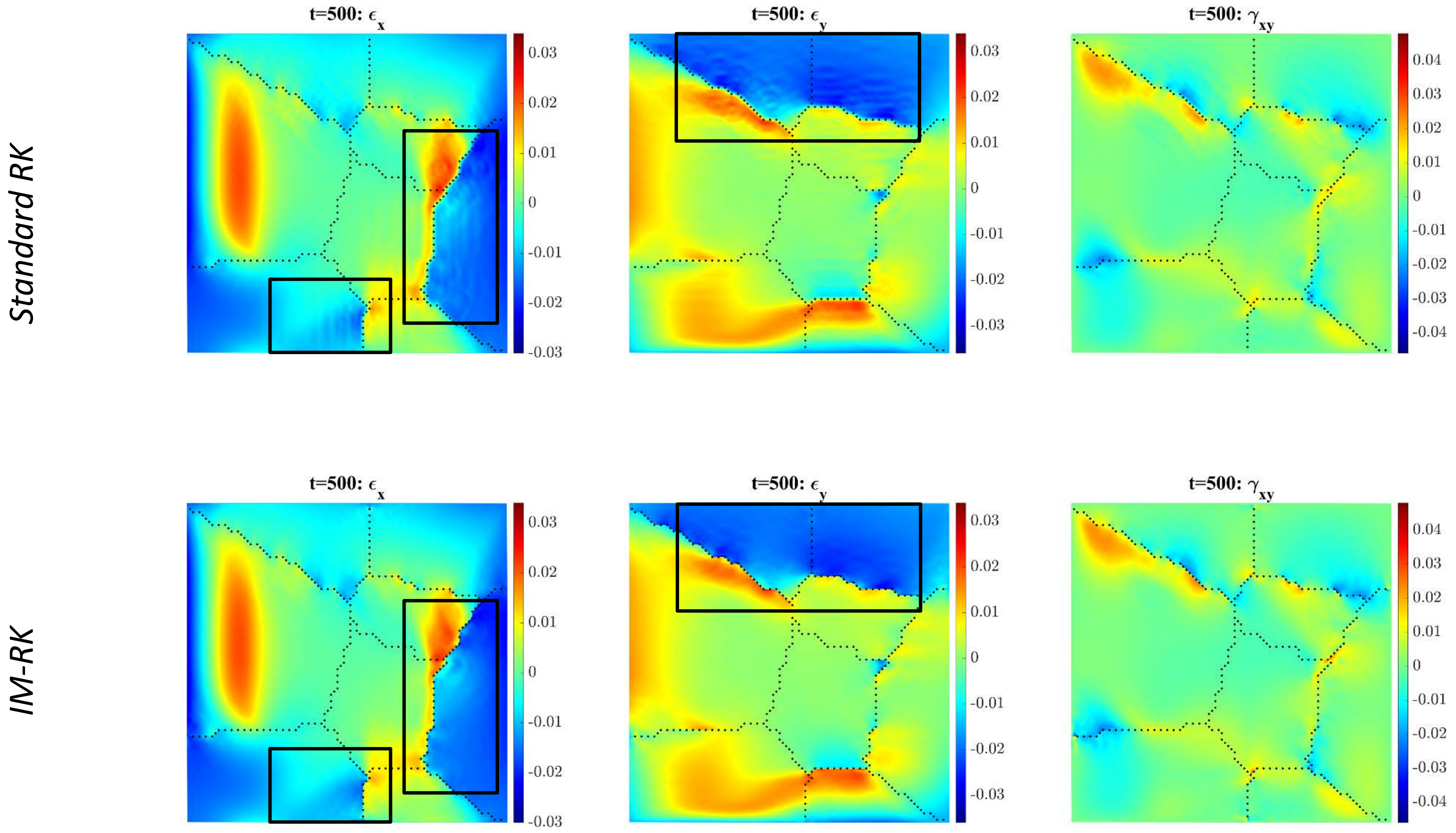

9. **Susuki, K.**, J. Allen, J.S. Chen. 2024. "Image-based Modeling of Coupled Electro-Chemo-Mechanical Behavior of Li-ion Battery Cathode Using an Interface-Modified Reproducing Kernel Particle Method." *Eng Comput* (Submitted)

Neural Network-Enhanced RKPM

Neural Network Enhanced Reproducing Kernel (NN-RK) Approximation

Solution decomposition

$$\mathbf{u}^h = \tilde{\mathbf{u}}^h + \hat{\mathbf{u}}^h$$

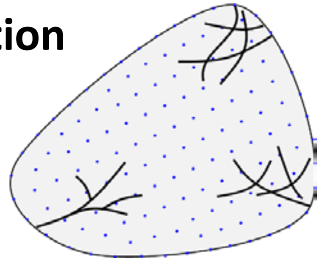

<u>**Smooth solution approximation**</u>

$$\tilde{\mathbf{u}}^h(\mathbf{X}) \approx \mathbf{u}^{RK}(\mathbf{X}) = \sum_{I=1}^{NP} \Psi_I(\mathbf{X})\mathbf{d}_I$$

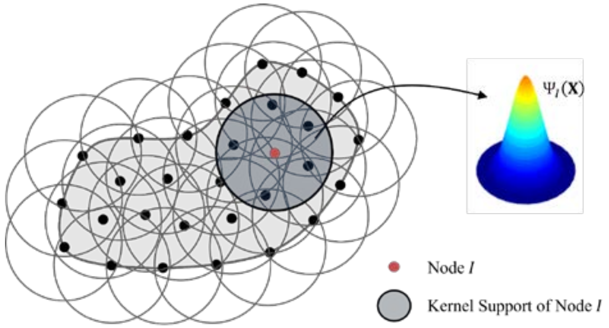

<u>**Neural Network (NN) Enrichment**</u>

$$\hat{\mathbf{u}}^h(\mathbf{x}) \approx \mathbf{u}^{NN}(\mathbf{X}) = \sum_{I=1}^{NB} b_I(\mathbf{X}; \mathbf{W})$$

Neural network (NN) approximation

$$u^{NN}(\mathbf{x}) = \sum_{B=1}^{N_B} b_B^{NN}(\mathbf{x}; \mathbf{W}_B)$$

- b_B^{NN}: block-level NN approximation

Block-level NN approximation

$$b_B^{NN}(\mathbf{x}; \mathbf{W}) = \sum_{K=1}^{N_K} \hat{\phi}_{KB}\left(\mathbf{y}(\mathbf{x}; \mathbf{W}_B^L), \mathbf{W}_{KB}^S\right) p(\mathbf{x}; \mathbf{W}_{KB}^P)$$

- NK: the number of NN kernels per block

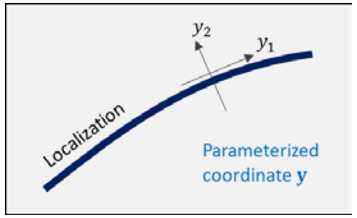

NN Kernel function captures
- Location and orientation of localization
- Shape of solution transition

NN Polynomial introduces
- Monomial completeness for further accuracy

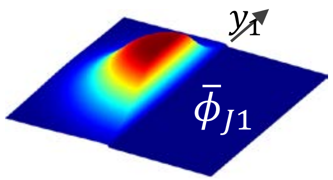

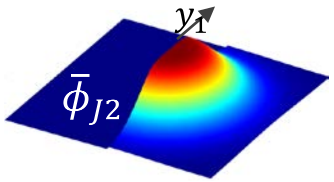

- $\mathbf{W}^L$: NN weight set controlling the location and orientation of the kernel.
- $\mathbf{W}^S$: NN weight set controlling the shape of transition.
- $\mathbf{W}^P$: NN monomial coefficient set

* The NN control parameters $\mathbf{W}^L$, $\mathbf{W}^S$, and $\mathbf{W}^P$ are ***automatically*** determined via loss function minimization.

12. Baek, J., J.S. Chen, **K. Susuki**. 2022. “A neural network-enhanced reproducing kernel particle method for modeling strain localization.” *Int J Numer Methods Eng* 123(18): 4422-4454.

Mixed-mode Fracture of Doubly Notched Crack Branching in Isotropic Media

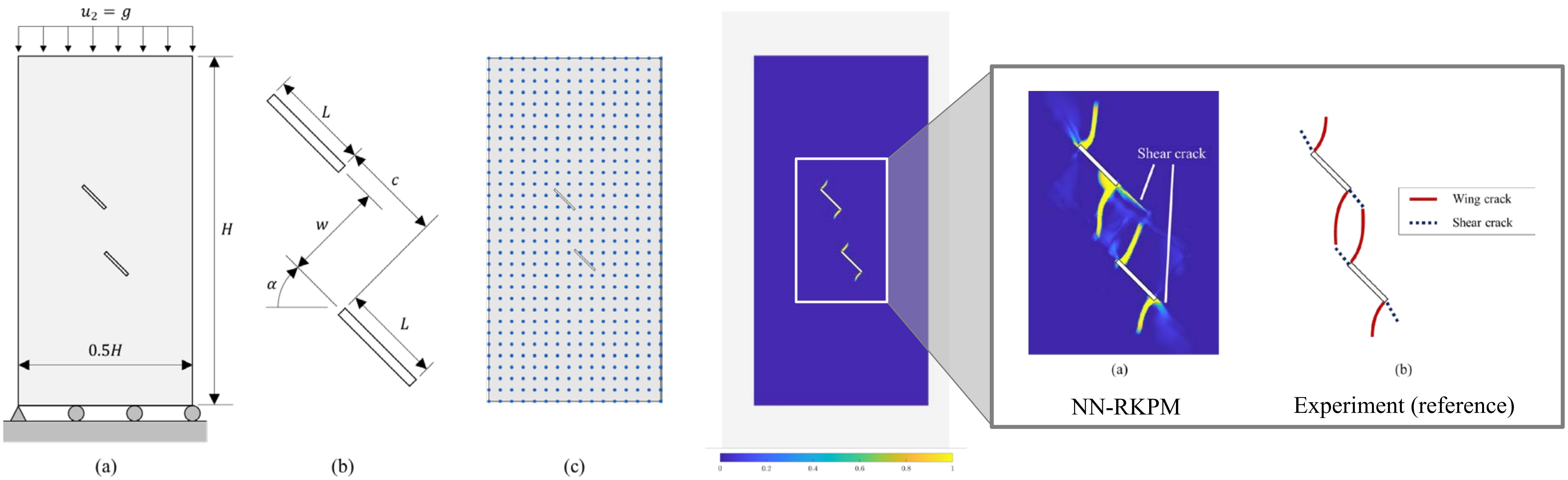

12. Baek, J., J.S. Chen, **K. Susuki**. 2022. "A neural network-enhanced reproducing kernel particle method for modeling strain localization." *Int J Numer Methods Eng*.
13. Baek, J., J.S. Chen. 2024. "A Neural Network-Based Enrichment of Reproducing Kernel Approximation for Modeling Brittle Fracture", *Comput Methods Appl Mech Eng*.
14. Bobet, A., H.H. Einstein, "Numerical modeling of fracture coalescence in a model rock material." *Int. J. Fract*. 92 (1998) 221–252.

Future Work: Approach for NNRK with Heterogeneous Media under Multi-Physics Loading

Coarse discretization for $\tilde{\mathbf{u}}^h$ with bulk material pixel point subset

Solution decomposition

$$\mathbf{u}^h = \tilde{\mathbf{u}}^h + \hat{\mathbf{u}}^h$$

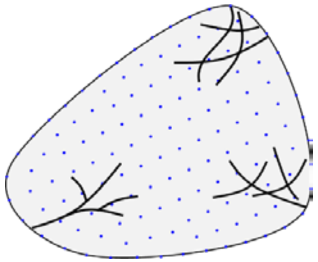

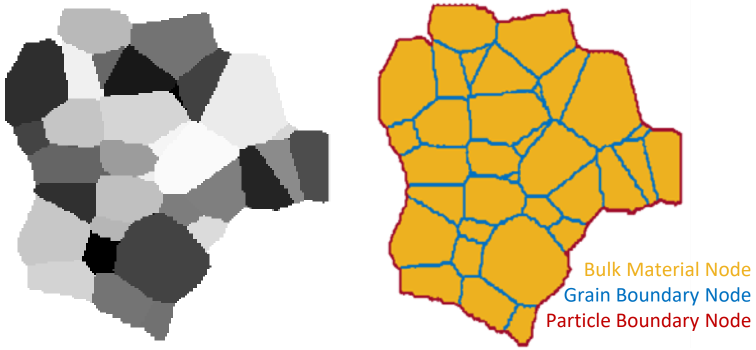

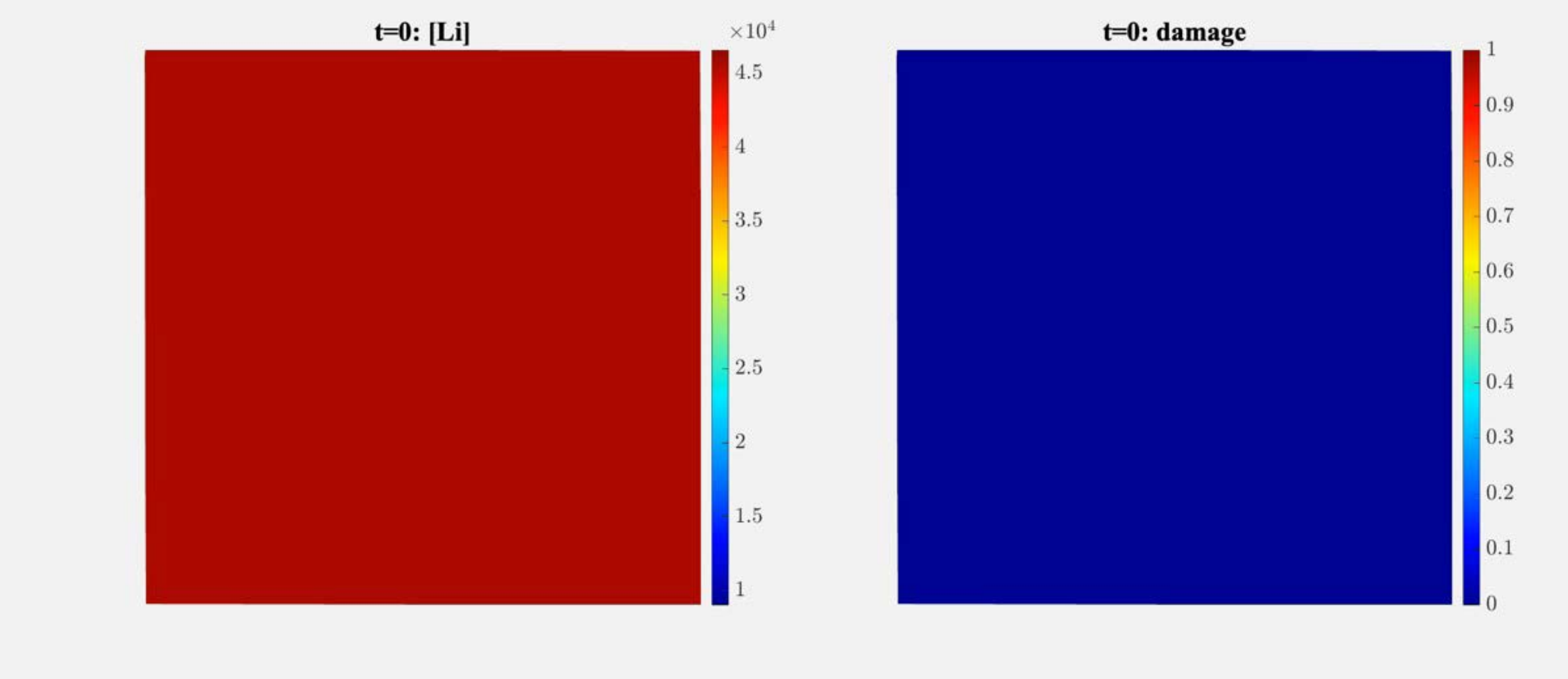

Conclusions

- A coupled linear patch test has been formulated and passed for the coupled electro-chemo-mechanical system, and optimal convergence rates are achieved.
- The interface-modified RK (IM-RK) approximation can introduce various discontinuities by leveraging kernel scaling and strategic interface node placement.
- IM-RK discontinuity introduction shows significant Gibbs oscillation reduction without additional degrees of freedom.
- NNRK is designed to be computationally efficient by superimposing a coarse solution with a localized NN enrichment for fine/localized features.
- NN block-level approximations are designed to capture low order topology but can be superimposed to capture complex topological geometries.

Thank you

Kristen Susuki – ksusuki@ucsd.edu

This work was authored in part by the National Renewable Energy Laboratory, operated by Alliance for Sustainable Energy, LLC, for the U.S. Department of Energy (DOE) under Contract No. DE-AC36-08GO28308. Funding provided by U.S. Department of Energy Office of Energy Efficiency and Renewable Energy. The views expressed in the article do not necessarily represent the views of the DOE or the U.S. Government. The U.S. Government retains and the publisher, by accepting the article for publication, acknowledges that the U.S. Government retains a nonexclusive, paid-up, irrevocable, worldwide license to publish or reproduce the published form of this work, or allow others to do so, for U.S. Government purposes.